L-304

NATIONAL ADVISORY COMMITTEE FOR AERONAUTICS

WARTIME REPORT

ORIGINALLY ISSUED
December 1942 as

~~Advance Restricted Report~~

THE EFFECT OF SOLIDITY, BLADE SECTION, AND CONTRAVANE

ANGLE ON THE CHARACTERISTICS OF AN AXIAL-FLOW FAN
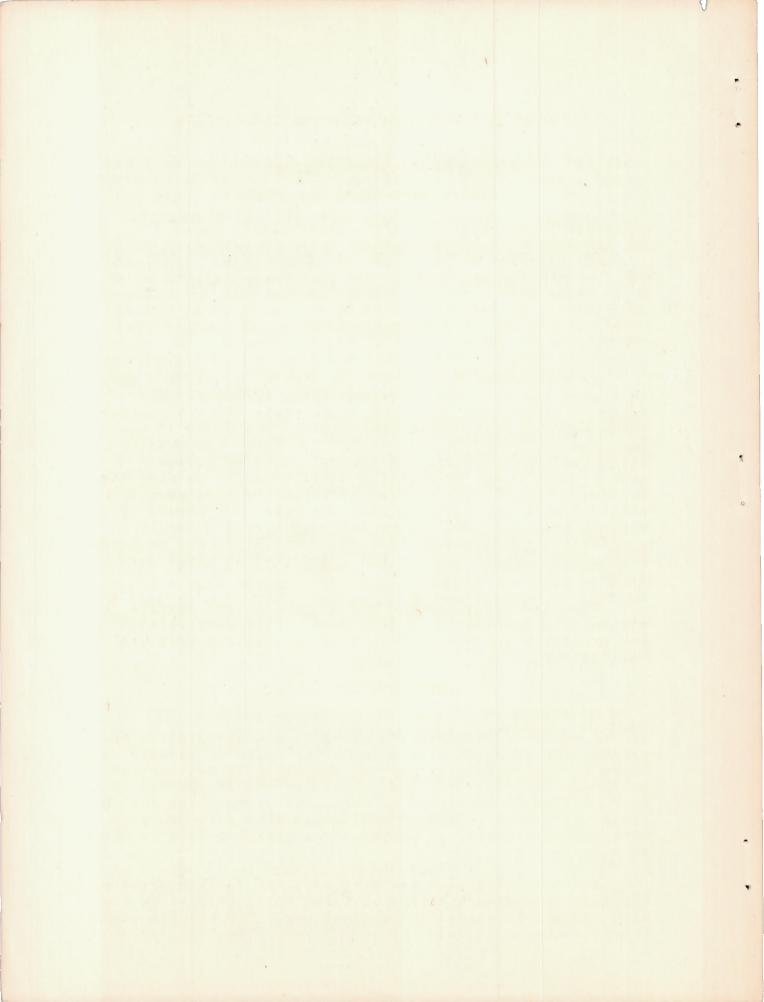
By E. Barton Bell and Lucas J. DeKoster

Langley Memorial Aeronautical Laboratory
Langley Field, Va.

CASE FILE
COPY

NACA

WASHINGTON

NATIONAL ADVISORY COMMITTEE FOR AERONAUTICS

ADVANCE RESTRICTED REPORT

THE EFFECT OF SOLIDITY, BLADE SECTION, AND CONTRAVANE

ANGLE ON THE CHARACTERISTICS OF AN AXIAL-FLOW FAN

By E. Barton Bell and Lucas J. DeKoster

SUMMARY

An axial-flow fan was tested with 6, 9, 12, 18, and 24 blades and with two different blade sections. The range of contravane angle and blade angle without contravanes was extended beyond the scope of the tests of the same fan published in NACA Report No. 729. The results indicated that suitable fan control could be achieved over a small range of quantity coefficient by varying the contravane angle; the highest efficiencies were usually obtained with the 12-blade fan; the rate of increase of maximum pressure coefficient and corresponding torque coefficient dropped with increasing solidity; and no large differences were found for the two different blade sections.

Formulas are developed for computing lift coefficients from fan-characteristic data. Lift coefficients are presented for the condition of maximum fan-pressure coefficient.

INTRODUCTION

A doctor's dissertation covering a comprehensive investigation of axial-flow fans on the basis of aerodynamic theory by Curt Keller was published in Switzerland in 1934. This material was translated and abstracted by Prof. Lionel S. Marks and is available to American designers in reference 1. The report of an extensive experimental investigation of single-stage axial blowers is given in reference 2.

In connection with tests of airplane cooling systems, the NACA conducted a series of tests on an axial-flow fan with adjustable blades and contravanes. The results were published as an advance restricted report in 1941, which

has been revised and published as reference 3. One fan with 24 blades of R.A.F. 6 section was tested over a limited range of blade and contravane settings.

Because of the possibility that greater efficiencies might be obtained with a smaller number of blades for fans handling a large volume of air at a low pressure rise, tests have now been made with four lower solidities. Some cooling and duct installations require a wide range of operating conditions that might be obtained by a change in blade angle. The mechanism required to control the blade angles in a many-blade hub leads, however, to serious mechanical complications and tests were included to show the effect of changing the angle of the contravanes to obtain this range of conditions.

The curves for the characteristics of a fan without contravanes have been extended to blade angles of 70° to cover the conditions that will be encountered in installations in which the blades are directly attached to the propeller spinner or make up the front fan of a dual-rotating pair.

The effect of airfoil section is shown by making additional tests with blades of NACA 6412 section. Airfoils of this section have the maximum camber slightly farther back from the leading edge than airfoils of R.A.F. 6 section and have a maximum lift coefficient of 1.67 as compared with 1.49 for the R.A.F. section.

SYMBOLS

The results given in this report are presented in terms of nondimensional coefficients, applicable to similar axial-flow fans.

These coefficients are defined as follows:

$$C_p = \frac{\Delta p}{\rho n^2 D^2} \qquad \text{pressure coefficient}$$

$$C_T = \frac{T}{\rho n^2 D^5} \qquad \text{torque coefficient}$$

$$\eta = \frac{1}{2\pi} \frac{C_p}{C_T} \frac{Q}{nD^3} \qquad \text{efficiency}$$

L-304

Q/nD^3 quantity coefficient

$$c_{T_v} = \frac{T_v}{\rho Q^2/D} \qquad \text{contravane torque coefficient}$$

$$C_L = \frac{2dL}{\rho w^2 \sigma_r dA} \qquad \text{lift coefficient}$$

where

Δp pressure rise across fan, pounds per square foot

ρ mass density of air, slugs per cubic foot

n rotational speed, revolutions per second

D fan diameter, feet

T torque, foot-pounds

Q quantity rate of flow, cubic feet per second

T_v torque on contravanes

L lift

w velocity relative to the blades

σ_r solidity at radius r $(Bb/2\pi r)$

A disk area

B number of blades

b blade width

r radius to any point

    The following additional symbols are used in the text and figures.

R radius to outside of fan $(D/2)$

r_o radius of hub $(0.69R)$

σ solidity $\left[\dfrac{Bb}{\pi R(1 + r_o/R)}\right]$

T_b torque on blades

T_s angular momentum in air stream

V velocity

Δp_b pressure increment across blades

Δp_v pressure increment across vanes

α stream angle between contravanes and blades, degrees

β blade angle at 0.714R, degrees

γ angle between lift and resultant-force vectors, degrees

θ angle between plane of rotation and velocity of air relative to blades, degrees

s angle of stagger, degrees

ϕ contravane angle at 0.714R, degrees

ψ final stream twist angle (average), degrees

APPARATUS

The test apparatus was essentially the same as that of reference 3. Figure 1 shows the hubs with the various numbers of blades. For the tests of five solidities a 24-blade hub was used with 24, 12, and 6 blades and an 18-blade hub was used with 18 and 9 blades. The corresponding solidities are:

Number of blades, B	Solidity, σ
6	0.21
9	.32
12	.43
18	.64
24	.86

In order to minimize the effects of unavoidable differences in blade setting, the tests for the highest

L-304

solidities were made first. Lower-solidity tests were
then made by removing the appropriate blades and substitut-
ing steel plugs, which gave surfaces flush with the hub.
The blades remaining for the low-solidity tests were thus
undisturbed from their original setting.

The original blades used in the fan in the tests re-
ported in reference 3 are of R.A.F. 6 section with a maxi-
mum thickness of 12 percent of the chord. Each blade has
a straight twist of 2° per inch of blade length and is not
tapered. For the tests reported herein, 24 additional
blades were made similar in all respects to the original
ones but of NACA 6412 airfoil section. (See fig. 2.)

TESTS

As in reference 3, all tests were run at a speed of
3600 rpm except for cases in which the torque would ex-
ceed 36.5 foot-pounds; tests in this range were run at
maximum torque.

With a blade angle of 25° and with the R.A.F. 6 blade
section, a series of tests was made for contravane angles
ranging from 40° to 115°. The angles were measured with
respect to a plane perpendicular to the axis of the fan.
Angles less than 90° indicate that the contravanes were
turning the air against the rotation of the blades; for
angles greater than 90° the air was turned in the direc-
tion of the blade rotation.

Tests were run at the five solidities for both air-
foil sections for blade angles of 25°, 35°, and 45° with-
out contravanes and for a blade angle of 25° with contra-
vanes set 70°.

Tests were also run with 24 blades and no contravanes
at blade angles from 20° to 70° for the R.A.F. 6 blade sec-
tion and from 20° to 65° for the NACA 6412 blade section.

RESULTS AND DISCUSSION

Extended contravane angles.- The results of the tests
on extended contravane angles are given in figures 3, 4,
and 5. Test points are omitted from these curves for the

sake of clarity. In figure 6 the values of C_p, C_T, η, and Q/nD^3 have been plotted against ϕ for the condition of maximum efficiency. The efficiency between the values of $\phi = 55^\circ$ and $\phi = 85^\circ$ is reasonably satisfactory. These same coefficients have been plotted in figure 7 for the condition of maximum C_p. There appears to be a stall in the contravanes at some point between $\phi = 50^\circ$ and $\phi = 40^\circ$. This stall has probably caused an excessive pressure drop through the contravanes and thereby decreased the fan pressure coefficient.

For a fan operating at a fixed Q/nD^3, considerable variation of pressure and torque can be obtained by varying the contravane angle. For example, a fan operating at a Q/nD^3 of 0.45 with 25° blade angle, the pressure coefficient can be varied from 2.46 at $\phi = 50^\circ$ to almost zero at $\phi = $ approximately 100°. There would, at the same time, be a decrease in torque coefficient from 0.228 at $\phi = 50^\circ$ to 0.06 at $\phi = $ approximately 100°. The efficiency will be greater than 80 percent between $\phi = 55^\circ$, $C_p = 2.35$ and $\phi = 79^\circ$, $C_p = 1.4$ and will drop off rapidly as ϕ increases. The torque and pressure, however, will also drop off rapidly, with the result that the wasted power is very small.

Although these tests have been run at only one blade angle, the same general trend would probably take place at any other blade angle. A fan designed with controllable contravanes would have a fairly satisfactory means of pressure control if the Q/nD^3 range were not too great.

Effect of solidity.- The results of the solidity tests are presented in figures 8 to 39. Curves for the R.A.F. 6 section are given in groups of three showing variation of C_p, C_T, and η with Q/nD^3 for different blade angles in figures 8 to 19; similar curves for the NACA 6412 section are given in figures 20 to 31. The variation with solidity σ of $C_{p_{max}}$, C_T, Q/nD^3, and η for the two sections are shown in figures 32 to 39.

The curves of C_p and C_T against Q/nD^3 for the different blade angles and both blade sections definitely show that the slope of these curves changes with solidity. The Q/nD^3 for $C_p = 0$ and $C_T = 0$ also decreases with increasing solidity. This decrease might be attributed to

the increased blocking of the larger number of blades. The best efficiencies were obtained for the 9- or 12- blade fan. In most cases the efficiency for the 24-blade fans was 4 or 5 percent less than the maximum. There was little difference between the two blade sections in the trend of efficiency for different numbers of blades. Figures 32 to 39 were cross-plotted from the other figures for the condition of maximum pressure coefficient. When these curves were cross-plotted, it was realized that the blade angles for the 18- and 9-blade tests might have been slightly different from the blade angles for the 24-, 12-, and 6-blade tests because of the difficulty of accurately setting the blades.

These curves show that while $C_{p_{max}}$ increases with solidity for all the cases tested, the slope of the curves is decreasing. Tests have not been made for a sufficiently high solidity to warrant the assumption that, beyond a certain solidity, no increase in pressure can be expected. With the exception of curves for $\beta = 45°$, no contravanes, the variation with solidity is practically the same for both blade sections. The efficiency at $C_{p_{max}}$ shows the value of contravanes at high solidity. At low solidities, higher efficiency is obtained without contravanes, because the contravanes absorb too large a part of the fan pressure rise.

Extended blade-angle test.- Figures 40, 41, and 42 show the fan characteristics without contravanes, with R.A.F. 6 blade sections, for blade angles from 20° to 70°. Similar results for the NACA 6412 blade section are shown in figures 43, 44, and 45. The curves are discontinued at the stall. For both blade sections, the maximum pressure comes at or near the stall up to $\beta = 55°$. Beyond $\beta = 55°$ the maximum pressure does not occur at the stall. There appears to be little choice between the two blade sections, either on the basis of maximum pressure or on the basis of efficiency. This statement cannot, however, be definitely made with respect to efficiency at the high blade angles, because the equipment did not permit the test to reach the point of maximum efficiency at angles above $\beta = 45°$.

Figures 46, 47, and 48 show the fan characteristics for operation with blades of NACA 6412 section at $\phi = 70°$. A comparison of these curves with those for the R.A.F. 6 blade section in reference 3 indicates a slightly

higher efficiency with the R.A.F. 6 blades and also a slightly higher maximum pressure except at high blade angles.

As a check on the method of measuring pressures, a manometer was connected to static orifices on each side of the fan. One side of the manometer was connected to an orifice in the outer fan casing upstream of the contravenes; the other side was connected to two orifices downstream of the fan. One orifice was in the outer casing and the other was in the cylindrical part of the hub fairing. Values of C_p were computed from the manometer readings and are plotted against Q/nD^3 in figure 49. The curve was obtained by the method described in reference 3. The orifices on the downstream side of the fan will give static pressure if there is no rotation in the air stream, and the manometer will then give the true pressure rise across the fan. From the stream angles for the condition $\beta = 25^\circ$, $\phi = 60^\circ$, the values from the manometer reading are seen to fall on the curve near the point where $\psi = 0^\circ$.

DETERMINATION OF LIFT COEFFICIENT

In order to calculate the lift coefficient of an airfoil, it is necessary to know the force on the airfoil and the direction and magnitude of the mean relative velocity. The vector diagrams for these forces and velocities are shown in figure 50. The determination of the lift coefficient of a blade section from fan characteristics must necessarily involve certain assumptions. These assumptions mainly concern the variation of velocity, torque, stream angle, and pressure along the radius. The velocity is assumed to be constant over the disk area. This assumption may be slightly in error due to effects of boundary layer and blade-pitch distribution, but it appears to be the most practical assumption. The torque loading is assumed to be constant over the disk area both for the contravenes and for the blades, that is, the torque per unit disk area is constant along the radius. From these assumptions and observations of the stream angle, a torque coefficient for the contravenes can be computed.

Determination of C_{T_v}.- The nondimensional coefficient is defined as

L-304

In order to determine C_{T_v}, it is therefore necessary to obtain T_v from the blower characteristics,

$$T_v = T_b - T_s$$

$$C_{T_v} = \frac{T_b}{\rho Q^2 / D} - \frac{T_s}{\rho Q^2 / D}$$

In order to evaluate T_s, the rotational momentum in the air stream is considered

$$T_s = \int_{r_o}^{R} rV \tan \psi \, \rho dQ$$

Substitution and integration give

$$T_s = \frac{2}{3\pi} \times \frac{[1 - (r_o/R)^3]}{[1 - (r_o/R)^2]^2} \times \frac{\rho Q^2}{R} \tan \psi$$

Evaluation of the constants, where $r_o/R = 0.69$, gives

$$T_s = 1.038 \frac{\rho Q^2}{D} \tan \psi$$

Therefore,

$$C_{T_v} = \frac{C_T}{(Q/nD^3)^2} - 1.038 \tan \psi \qquad (1)$$

The contravane torque coefficient C_{T_v} was computed from equation (1) for each test point of the runs with contravanes. These points were then arithmetically averaged for each contravane angle. The averages of these readings are plotted as points on the curve of figure 51. A faired curve was then drawn through the points and values from the faired curve were used in further calculations.

In the calculations of the lift coefficients, some operating condition must be chosen. In connection with fan design, the condition of maximum pressure is the chief point of interest. In most cases the maximum pressure occurred at or near the stall. It was therefore decided to compute the C_L of the blades for the condition of $C_{p_{max}}$.

Determination of C_L from torque considerations.— Consider the increment of lift dL on an annulus of area dA at radius r,

$$C_L = \frac{2dL}{\rho w^2 \sigma_r dA}$$

$$dL = \frac{dT_b}{r} \times \frac{\cos \gamma}{\sin(\theta + \gamma)}$$

If it is assumed that $dT_b = \frac{T_b}{A} dA$

$$C_L = \frac{2T_b dA}{A r \rho w^2 \sigma_r dA} \times \frac{\cos \gamma}{\sin(\theta + \gamma)}$$

$$C_L = 2\pi \left(1 - \frac{r_o}{R}\right) \times \frac{C_T}{\sigma (Q/nD^3)^2} \times \frac{\sin^2 \theta \cos \gamma}{\sin(\theta + \gamma)}$$

Evaluation of the constants where $r_o/R = 0.69$ gives

$$C_L = \frac{1.948 \, C_T}{\sigma (Q/nD^3)^2} \times \frac{\sin \theta \tan \theta}{\tan \theta + \tan \gamma} \qquad (2)$$

Tan θ is determined as follows:

$$\tan \theta = \frac{V}{\pi n D \frac{r}{R} + \frac{1}{2}(V \tan \alpha - V \tan \psi)}$$

$$\tan \theta = \frac{2}{\frac{\pi^2}{2}\left[1 - \left(\frac{r_o}{R}\right)^2\right] \frac{r}{R} \frac{1}{Q/nD^3} + \tan \alpha - \tan \psi}$$

$$\tan \theta = \frac{2}{2.586 \frac{r}{R} \frac{1}{Q/nD^3} + \tan \alpha - \tan \psi} \qquad (3)$$

In order to determine $\tan \alpha$, consider an annulus of area dA at a radius r on the contravanes,

$$dT_v = \frac{T_v}{A} \, dA$$

$$dT_v = \frac{T_v}{A} \times 2\pi r \, dr$$

But from consideration of the rotational momentum,
$dT_v = rV \tan \alpha \, \rho dQ$,

$$\tan \alpha = \frac{T_v}{rV\rho Q}$$

$$\tan \alpha = \frac{\pi}{2} \left[1 - \left(\frac{r_0}{R} \right)^2 \right] \left(\frac{C_{T_v}}{r/R} \right)$$

$$\tan \alpha = \frac{0.823 \, C_{T_v}}{r/R} \tag{4}$$

For the operation without contravanes, an annulus at radius r is considered and $\tan \psi$ is computed as follows:

$$dT_b = dT_s$$

$$dT_b = \frac{T_b}{A} \times 2\pi r \, dr$$

From momentum considerations, $dT_s = rV \tan \psi \, \rho dQ$

$$\tan \psi = \frac{T_b}{rV\rho Q}$$

$$\tan \psi = \frac{\pi}{2} \left[1 - \left(\frac{r_0}{R} \right)^2 \right] \frac{1}{r/R} \times \frac{C_T}{(Q/nD^3)^2}$$

$$\tan \psi = 0.823 \, \frac{1}{r/R} \times \frac{C_T}{(Q/nD^3)^2} \tag{5}$$

For operation with contravanes, the contravane torque coefficient was developed from observed values of ψ by

equation (1). Rearranging this equation and substituting it in equation (5) for conditions of $C_{T_V} = 0$ gives

$$0.823 \; \frac{C_T}{\frac{r}{R} \, (Q/nD^3)^2} = \frac{C_T}{(Q/nD^3)^2} \times \frac{1}{1.038}$$

$$r/R = 0.854$$

The direction of the inflow velocity is computed from C_{T_V} by equation (4), which gives the stream angle ahead of the blades α as a function of r/R. This equation is rigorous only for the condition at which the blades have the proper pitch distribution to give a constant torque disk loading. When $C_{T_V} = 0$, for example, the equation would indicate that $\alpha = 0$ for all r/R values. But, because the twist in the blades is unchanged from the design operating conditions, the angle will be negative at the root and positive at the tip. At some particular radius, however, the angle will be zero, as indicated by equation (4). The computed final stream angle ψ is also assumed constant along the radius. This assumption will be true for $\psi = 0$. At other computed values of ψ, this assumption will not be true but ψ will vary along the radius, and the computed value will be the mean value. Without contravanes this distribution along the blades can be computed from equation (5). If the two expressions for final stream angle are equated for $C_{T_V} = 0$, a value of $r/R = 0.854$ is found for which equation (1) will give the same stream angle as computed from equation (5). At this radius, the values of ψ as computed from equation (5), and α as computed from equation (4) will be approximately correct for all values of ϕ. This value of r/R is approximately equal to the value of r/R for which the outside and inside disk areas are equal. The value for equal areas is $r/R = 0.859$. Consequently, a value of $r/R = 0.86$ was selected as the station for which to compute the value of C_L.

In the computation of the lift coefficients for maximum pressure coefficient, the values of C_T, C_p, and Q/nD^3 were picked from the fan curves. These values were plotted against β for condition of constant ϕ and σ, against ϕ for constant β and σ, and against σ for constant ϕ and β. Values were picked off these faired curves from which to compute C_L. In all cases ψ

was computed from the value of C_{T_V} by equation (1) or by equation (5). A value of $\tan \gamma = 0.06$ was arbitrarily assumed. This assumption may be in error but is of secondary importance because it does not materially affect the value of C_L.

The computed values of C_L are plotted for various solidities against the stagger angle s in figures 52 to 55. The stagger angle s is defined as the angle between the incoming air and the plane of the blades.

$$\tan s = \frac{V}{\pi n D \dfrac{r}{R} + V \tan \alpha}$$

$$\tan s = \frac{1}{\dfrac{\pi^2}{4}\left[1 - \left(\dfrac{r_o}{R}\right)^2\right]\dfrac{r}{R} \times \dfrac{1}{Q/nD^3} + \tan \alpha}$$

$$\tan s = \frac{1}{1.293 \dfrac{r}{R} \dfrac{1}{Q/nD^3} + \tan \alpha} \tag{6}$$

Determination of C_L from pressure coefficients.- The lift coefficient on the blades may also be computed from consideration of the pressure measurements. The pressure rise across the blades is not, however, the total pressure rise across the fan but is equal to the pressure rise across the fan plus the pressure drop across the contra-vanes,

$$\Delta p_b = \Delta p + \Delta p_v$$

If an annulus of the fan at radius r is considered,

$$C_L = \frac{2 dL}{\rho w^2 \sigma_r dA}$$

$$dL = \Delta p_b \, dA \, \frac{\cos \gamma}{\cos (\theta + \gamma)}$$

$$C_L = \frac{2 \Delta p_b \, dA}{\rho w^2 \sigma_r dA} \times \frac{\cos \gamma}{\cos (\theta + \gamma)}$$

$$C_L = \frac{2r/R}{\sigma \left(1 + \frac{r_o}{R}\right)} \left\{ \frac{\pi^2}{8} \left[1 - \left(\frac{r_o}{R}\right)^2\right]^2 \frac{C_p}{(Q/nD^3)^2} + \frac{1}{\cos^2 \alpha} - 1\right\} \frac{\sin^2 \theta \cos \gamma}{\cos(\theta + \gamma)}$$

Evaluation of the constants $(r_o/R = 0.69)$ gives

$$C_L = 1.18 \frac{r/R}{\sigma} \left[0.339 \frac{C_p}{(Q/nD^3)^2} + \frac{1}{\cos^2 \alpha} - 1\right] \frac{\tan \theta \sin \theta}{1 - \tan \theta \tan \gamma} \qquad (7)$$

For the condition of no contravanes, $\alpha = 0$,

$$C_L = 0.40 \frac{r/R}{\sigma} \times \frac{C_p}{(Q/nD^3)^2} \times \frac{\tan \theta \sin \theta}{1 - \tan \theta \tan \gamma} \qquad (8)$$

The values of C_L as computed from equation (8) are also plotted in figures 52 to 55. This method of computing C_L from pressure characteristics is probably not so accurate as the method from torque characteristics. In the method of computing C_L from pressure coefficients the assumption is made that both the pressure and torque loading are constant over the disk area. The calculation of pressure drop through the contravanes neglects the drag of the contravanes.

If the two blade sections tested are compared on the basis of computed lift coefficients, the curves of figures 52 and 54 show that the NACA 6412 section gives a higher C_L at the upper end of the stagger-angle range; whereas the values are nearly equal or slightly higher for the R.A.F. 6 blade section at stagger angles below about 16° to 24°, depending on the solidity.

In figure 53, the four points plotted at stagger angles below 2° do not seem consistent with the rest of the curve. These values were taken from tests at blade angles of 10° and 15°. At these low blade angles, there is no definite stall and no true maximum C_p. The stagger angle cannot be small enough actually to stall the blades. The maximum limit on the angle between the blade and the incoming air $(\beta - s)$ is equal to β when $s = 0$,

L-304

which is the condition of $Q/nD^3 = 0$. The angle of the air approaching the blades, therefore, cannot become large enough to stall them. When $Q/nD^3 = 0$, the lift coefficient is indeterminate if any pressure is developed or torque is absorbed. The basic assumptions for computing C_L become invalid as this condition is approached. The foregoing derivations for lift coefficients are thus seen to break down at low values of Q/nD^3. Pressure that is produced with no air flow through the fan is evidently the result of a circulation around each individual blade.

The excessive scatter of points for the data taken from tests with contravanes, as shown in figures 52 and 53, is probably due to variation from the assumed distributions of velocity, pressure, and torque. In most cases the agreement between calculations from pressure curves and torque curves is satisfactory.

There is need for additional data from airfoil cascade tests with respect to lift coefficient and angle of attack, from zero lift to the stall and beyond to a point corresponding to zero quantity, for various solidities and various airfoil sections.

SUMMARY OF RESULTS
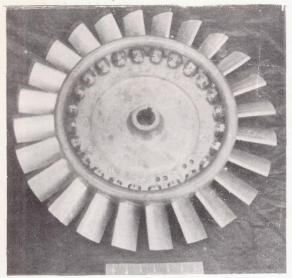
Tests of an axial-flow fan with 6, 9, 12, 18, and 24 blades of R.A.F. 6 and NACA 6412 airfoil section through a range of contravane and blade angles indicate:

1. A change in the contravane angle was a suitable means of controlling the pressure output of a fan when the quantity range of operation was small.

2. The 12-blade fan gave the highest efficiencies in nearly all cases.

3. The drag of the contravanes caused a falling off of the efficiency at low solidities.

4. The angle of attack for zero pressure and torque decreased with increasing solidity.

5. No large differences appeared in the characteristics of a fan with blades of R.A.F. 6 section and of NACA 6412 section.
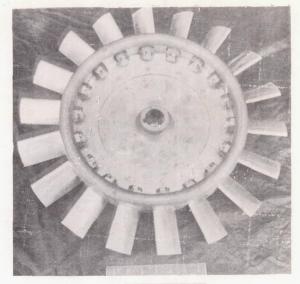
6. The NACA 6412 section showed a slightly higher computed lift coefficient than the R.A.F. 6 section for most conditions, but the difference was not of the order indicated by conventional airfoil tests.

7. At maximum pressure coefficient the lift coefficient considerably decreased with increasing solidity.

Langley Memorial Aeronautical Laboratory,
    National Advisory Committee for Aeronautics,
        Langley Field, Va.

REFERENCES
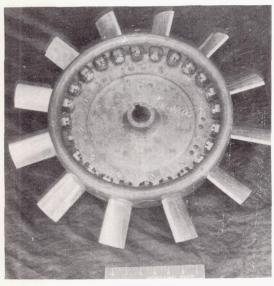
1. Keller, Curt: The Theory and Performance of Axial-Flow Fans. First ed., McGraw-Hill Book Co., Inc., 1937.

2. Ruden, P.: Investigation of Single Stage Axial Fans. NACA TM No. 1062, 1944.

3. Bell, E. Barton: Test of a Single-Stage Axial-Flow Fan. NACA Rep. No. 729, 1942.

$\sigma = 0.86$

$\sigma = 0.64$

$\sigma = 0.43$

$\sigma = 0.32$
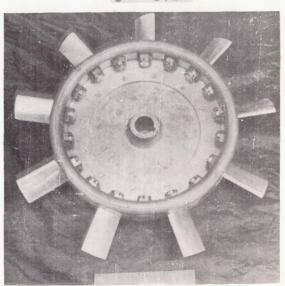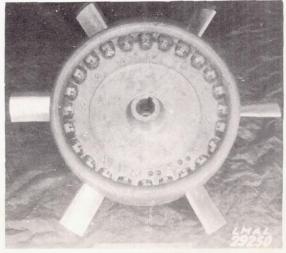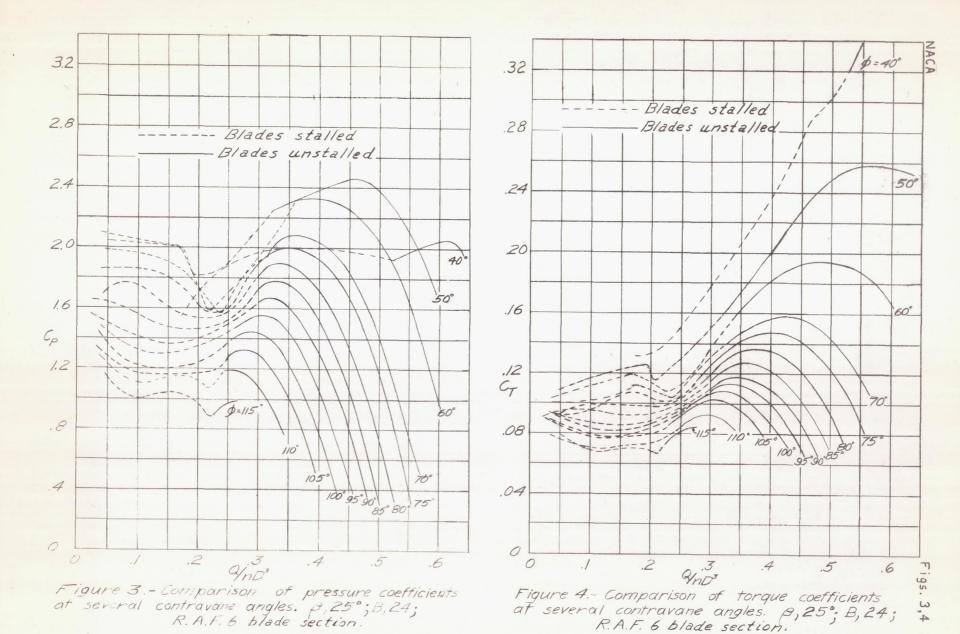
$\sigma = 0.21$

Figure 1.- Fan wheels of various solidities.

STATION	ORDINATES	
	UPPER	LOWER
0	0	0
.050	.0760	-.0330
.100	.1070	-.0400
.200	.1515	-.0400
.400	.2070	-.0250
.600	.2330	-.0075
.800	.2360	.0040
1.000	.2230	.0110
1.200	.1990	.0155
1.400	.1645	.0170
1.600	.1205	.0145
1.800	.0665	.0080
2.000	.0025	-.0025
L.E.R.	.0315	
T.E.R.	.0025	
SLOPE OF L.E. RADIUS THROUGH END OF CHORD: 6/20		

NACA

6° STRAIGHT TWIST

VIEW AA

10½"R

3"

4⅞"

3¼"

1¾" DIAM.

.10"

SECTION BB

1"   1"

Figure 2.- Axial fan blade with NACA 6412 section

Fig. 2

Figure 3.- Comparison of pressure coefficients at several contravane angles. β,25°; B,24; R.A.F. 6 blade section.

Figure 4.- Comparison of torque coefficients at several contravane angles. β,25°; B,24; R.A.F. 6 blade section.

NACA

Figure 5.- Efficiencies at several contra vane angles. β,25°; B,24; R.A.F. 6 blade section.

Figure 8.- Pressure coefficients at various solidities. β,25°; φ,70°; R.A.F. 6 blade section.

Fig. 6
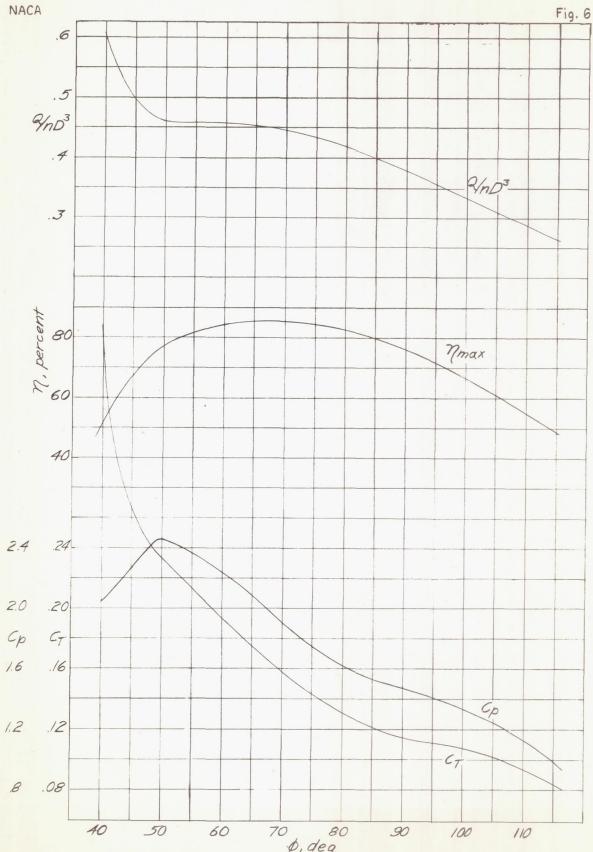
Figure 6.— Fan characteristics for maximum efficiency. β, 25°; B, 24; R.A.F. 6 blade section.

L-304
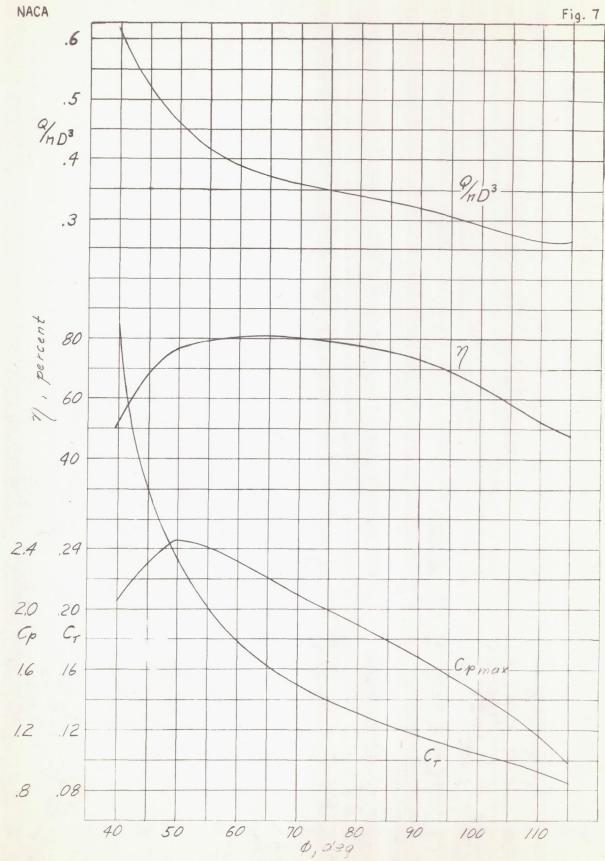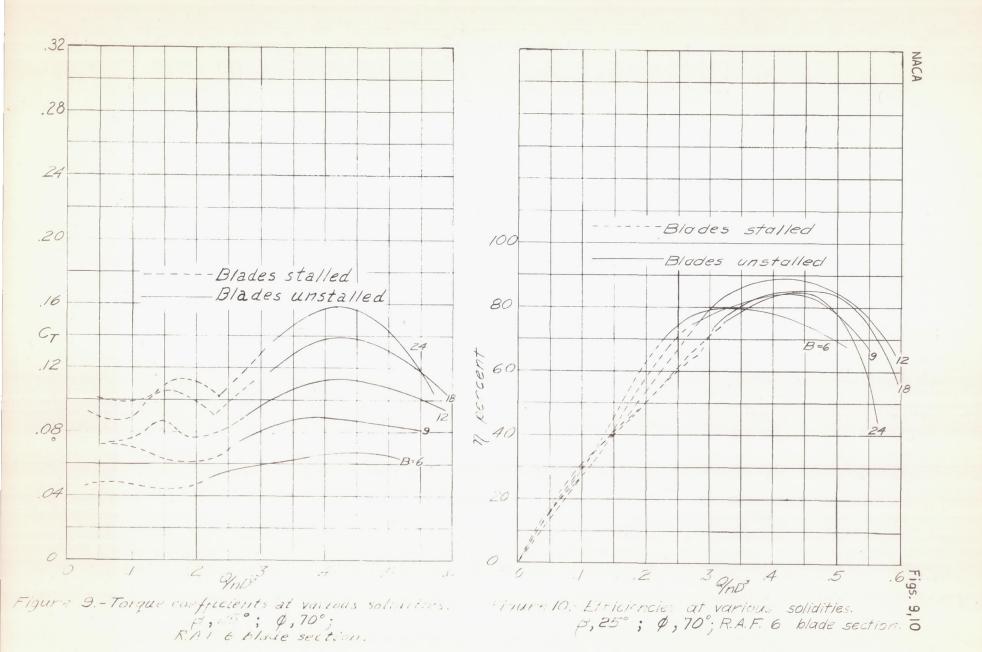
Figure 7.— Fan characteristics for maximum pressure
        coefficient. β, 25°; β, 24; R.A.F. 6 blade section.
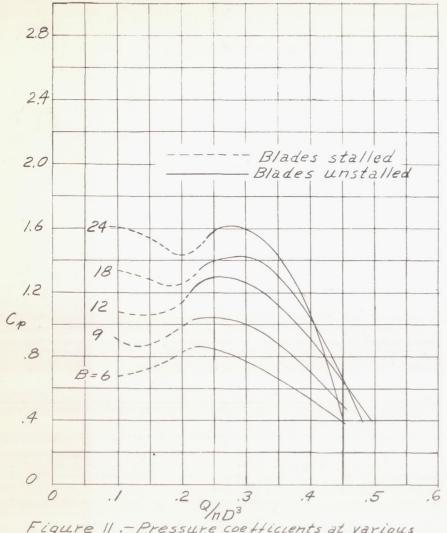
Figure 9.- Torque coefficients at various solidities.
β, 25°; φ, 70°;
R.A.F. 6 blade section.

Figure 10.- Efficiencies at various solidities.
β, 25°; φ, 70°; R.A.F. 6 blade section.

Figure 11.— Pressure coefficients at various solidities. β, 25°; no contravanes; R.A.F. 6 blade section.
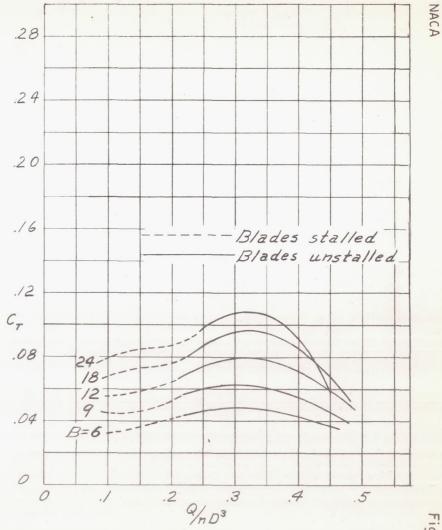
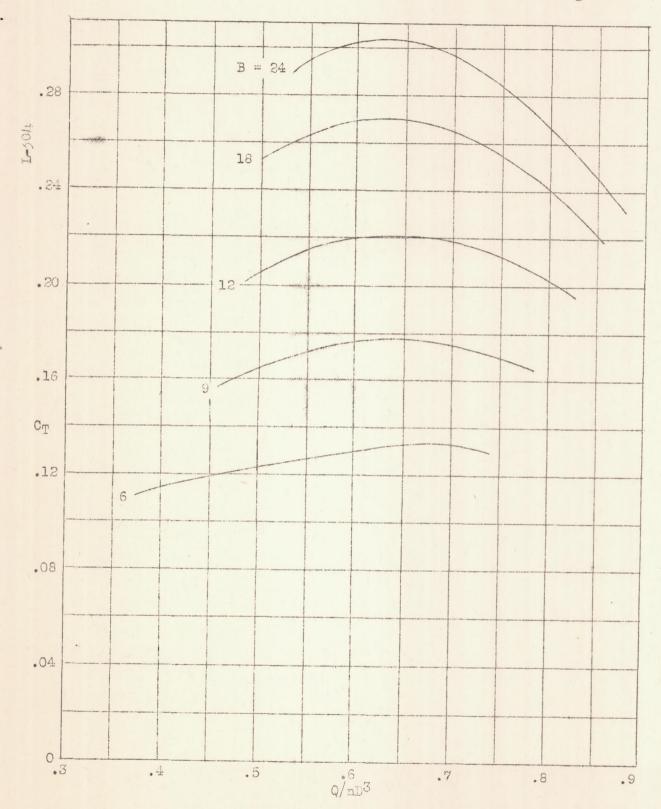Figure 12.— Torque coefficients at various solidities. β, 25°; no contravanes; R.A.F. 6 blade section.
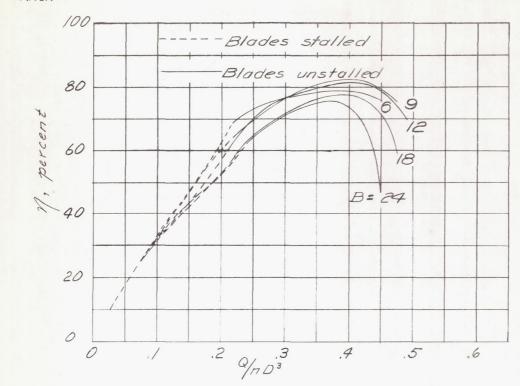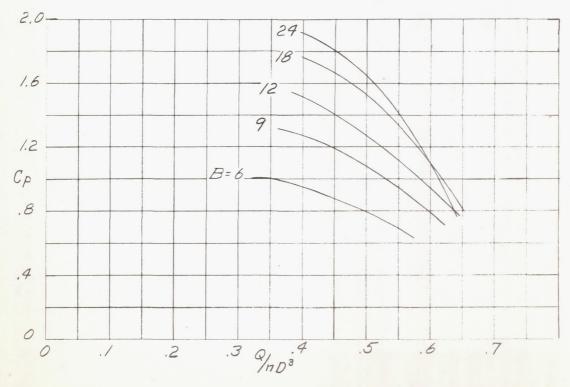
Figure 13.— Efficiencies at various solidities.
β, 25°; no contravanes;
R.A.F. 6 blade section.

Figure 14.— Pressure coefficients at various solidities.
β, 35°; no contravanes; R.A.F. 6 blade section.
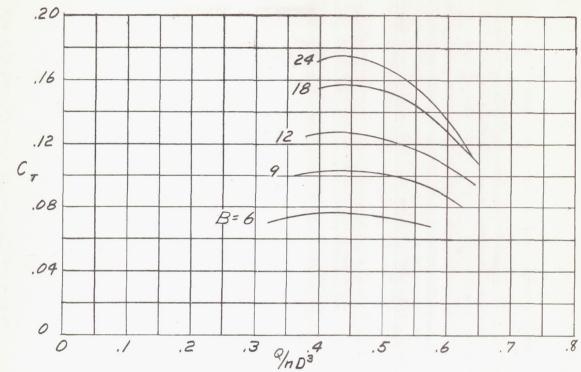
Figure 15.— Torque coefficients at various solidities.
β, 35°; no contravanes; R.A.F. 6 blade section.
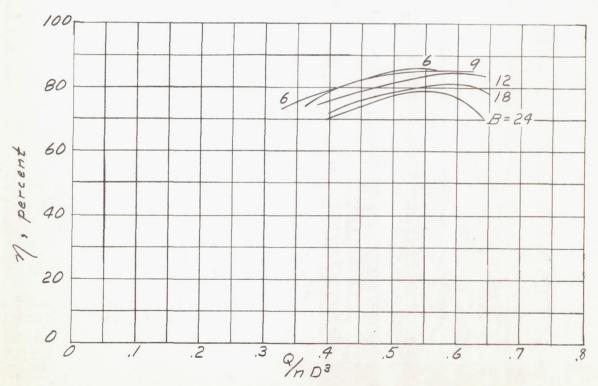
Figure 16.— Efficiencies at various solidities.
β, 35°; no contravanes;
R.A.F. 6 blade section.
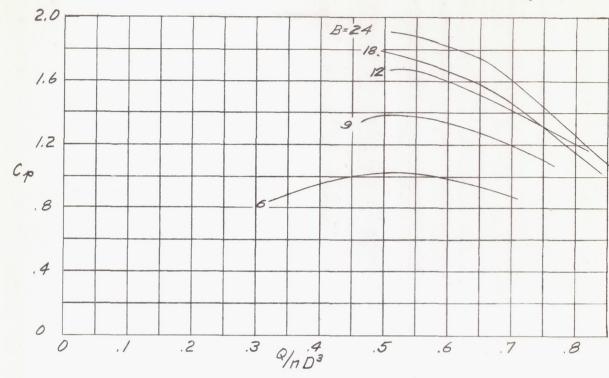
Figure 17.— Pressure coefficients at various solidities.
β, 45°; no contravanes; R.A.F. 6 blade section.
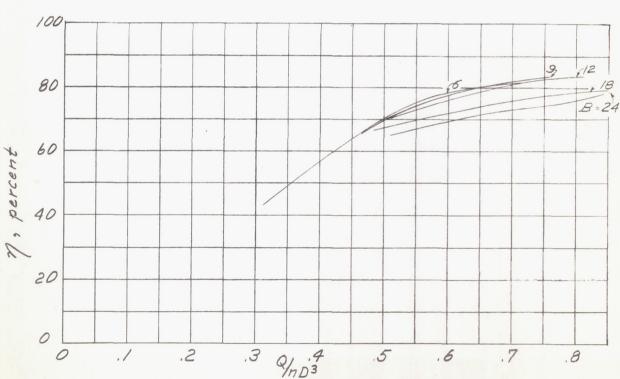
Figure 19.— Efficiencies at various solidities.
β, 45°; no contravanes;
R.A.F. 6 blade section.

Figure 18.- Torque coefficients at various solidities. $\beta = 45°$, no contravanes. R.A.F. 6-blade section.
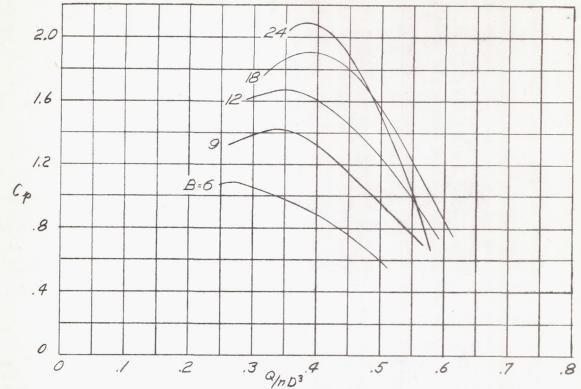
Figure 20.—Pressure coefficients at various solidities.
ϕ, 70°; β, 25°; NACA 6412 blade section.
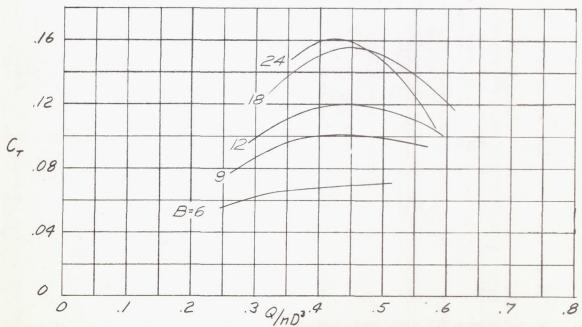
Figure 21.—Torque coefficients at various solidities.
ϕ, 70°; β, 25°; NACA 6412 blade section.

L-304
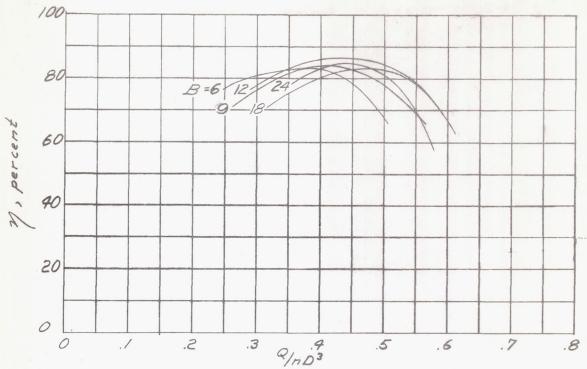
Figure 22.—Efficiencies at various solidities. ϕ, 70°; β, 25°; NACA 6412 blade section.

Figure 23.—Pressure coefficients at various solidities. β, 25°; no contravanes; NACA 6412 blade section.

L-304
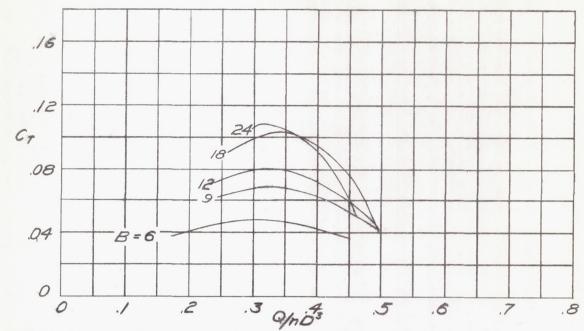
Figure 24.- Torque coefficients at various solidities.
β, 25°; no contravanes; NACA 6412 blade section.
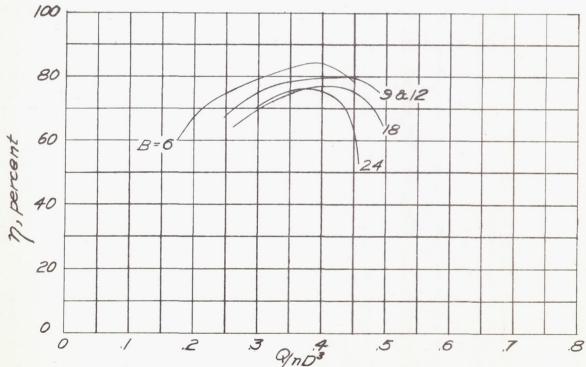
Figure 25.- Efficiencies at various solidities.
β, 25°; no contravanes; NACA 6412 blade section.

L-304
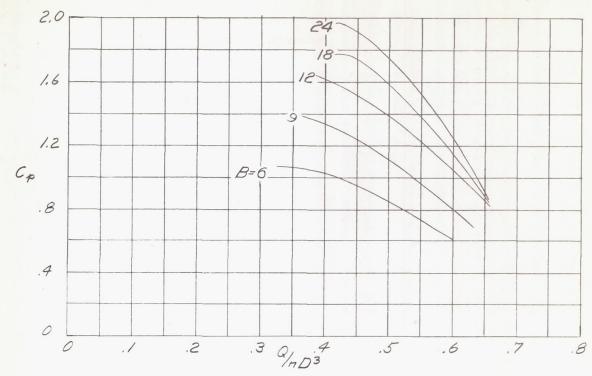
Figure 26.— Pressure coefficients at various solidities.
β, 35°; no contravanes; NACA 6412 blade section.
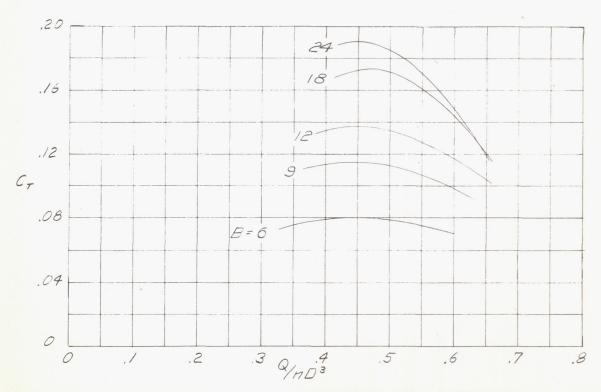
Figure 27.— Torque coefficients at various solidities.
β, 35°; no contravanes; NACA 6412 blade section.

L-304
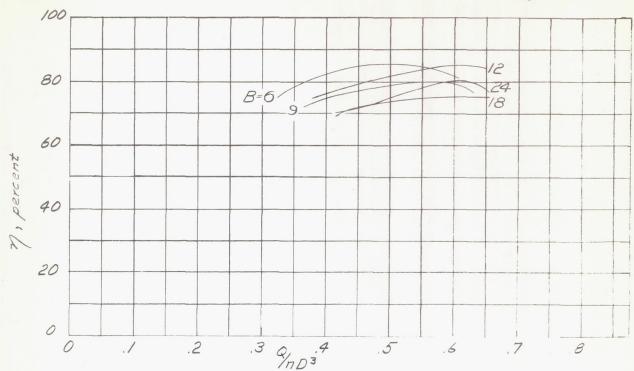
Figure 28.— Efficiencies at various solidities.
    β, 35°; no contravanes; NACA 6412 blade section.
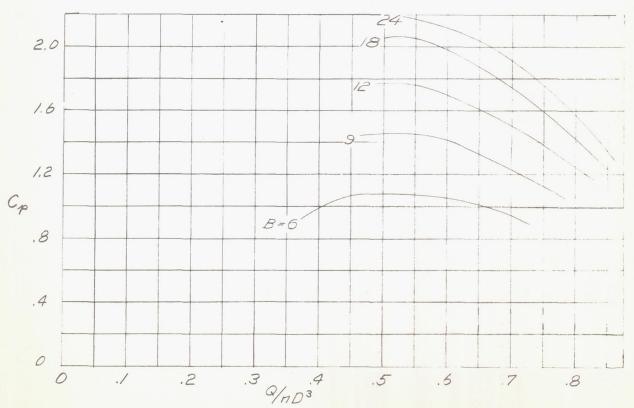
Figure 29.— Pressure coefficients at various solidities.
    β, 45°; no contravanes; NACA 6412 blade section.

Figure 30.— Torque coefficients at various solidities. β = 45°, no contravanes. NACA 6412 blade section.

L-304
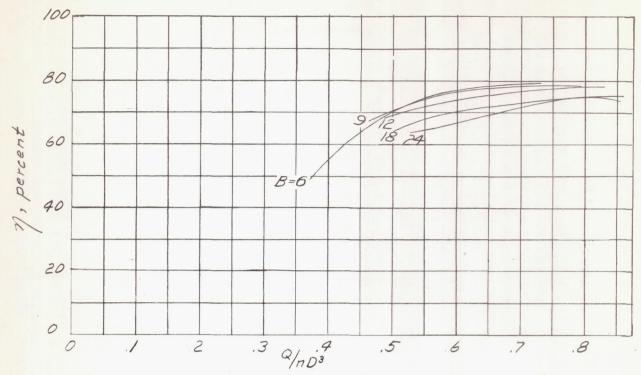
Figure 31.- Efficiencies at various solidities.
β, 45°; no contravanes; NACA 6412 blade section.
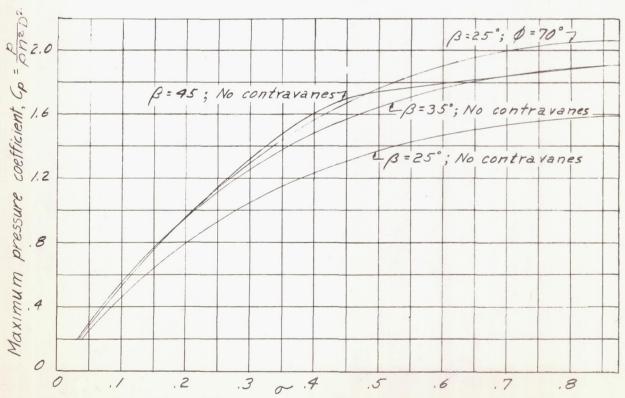
Figure 32.- Maximum pressure coefficients.
R.A.F. 6 blade section.
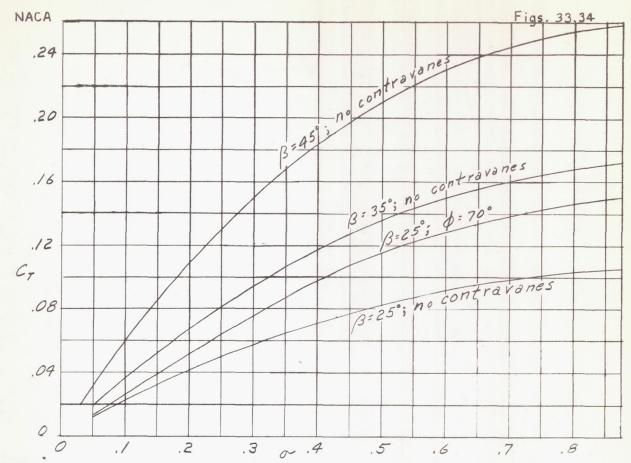
Figure 33.— Torque coefficients at maximum pressure coefficients.
R.A.F. 6 blade section.
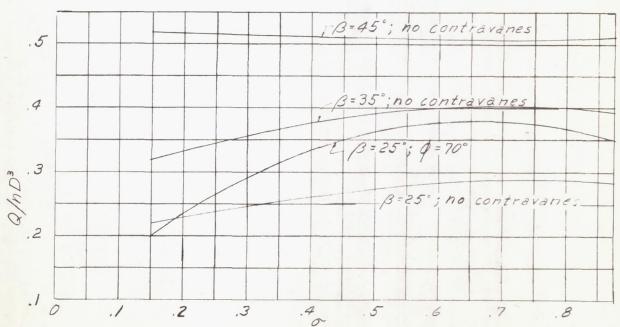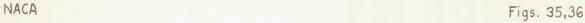
Figure 34.— Quantity coefficients at maximum pressure coefficients.
R.A.F. 6 blade section.
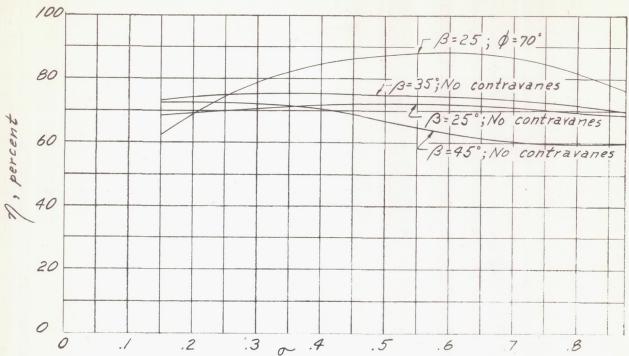
Figure 35.- Efficiencies at maximum pressure coefficient.
R.A.F. 6 blade section.
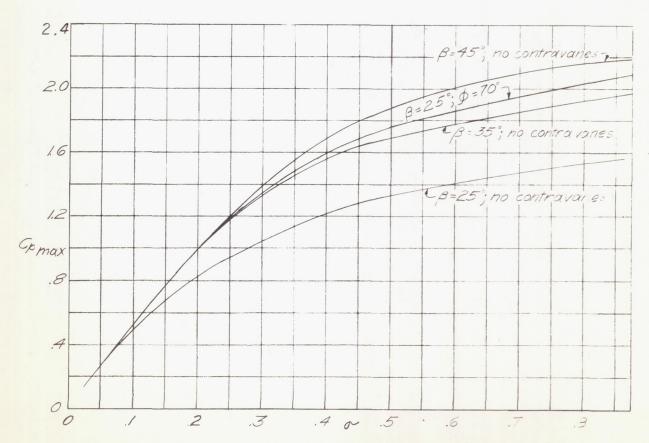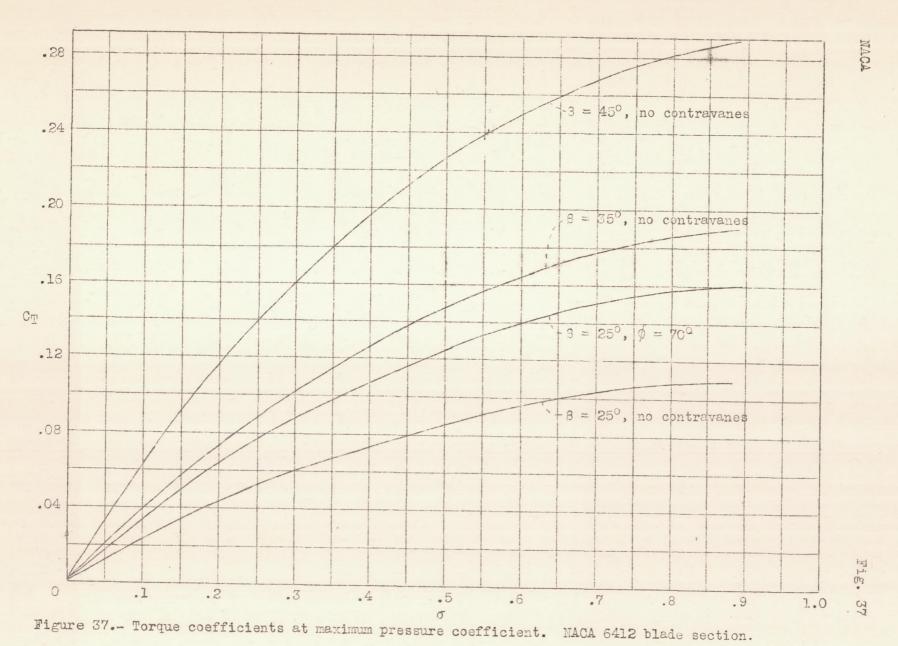
Figure 36.- Maximum pressure coefficients. NACA 6412 blade
section.

Figure 37.— Torque coefficients at maximum pressure coefficient.   NACA 6412 blade section.

Fig. 37
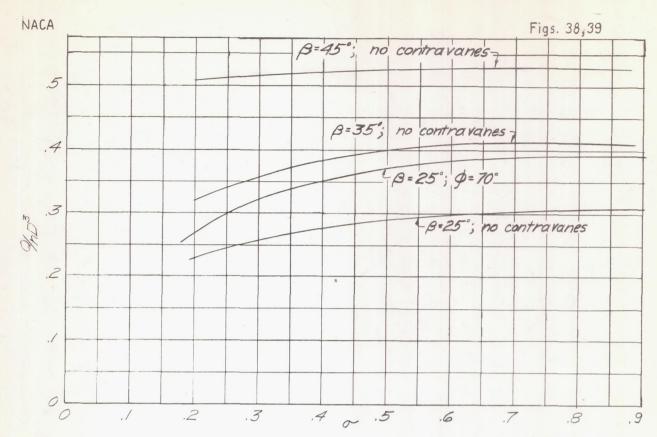
Figure 38.- Quantity coefficient at maximum pressure coefficient.
NACA 6412 blade section.
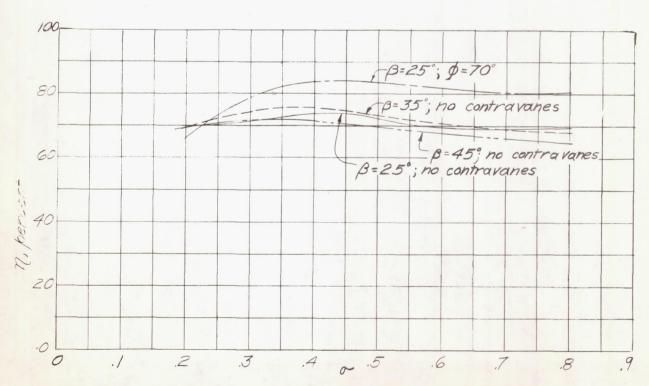
Figure 39.- Efficiencies at maximum pressure coefficient.
NACA 6412 blade section.

L-304
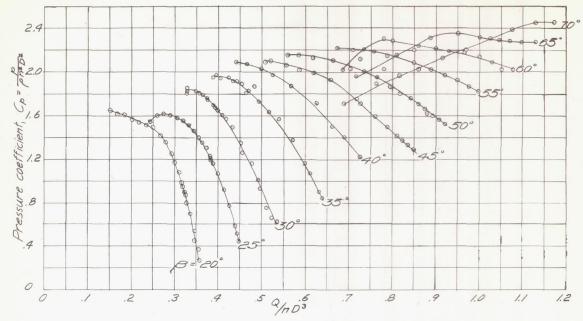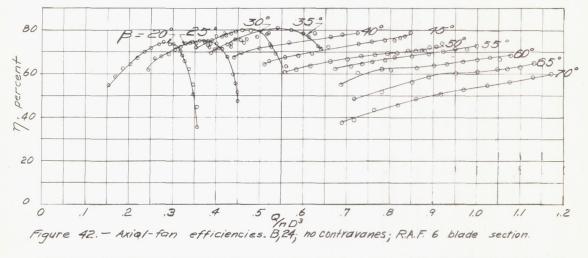
Figure 40.— Pressure coefficients. B,24; no contravanes; R.A.F. 6 blade section.

Figure 42.— Axial-fan efficiencies. B,24; no contravanes; R.A.F. 6 blade section.
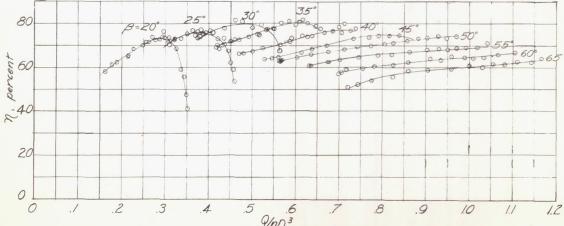
Figure 45.—Axial-fan efficiencies; No contravanes; B,24; NACA 6412 blade section.
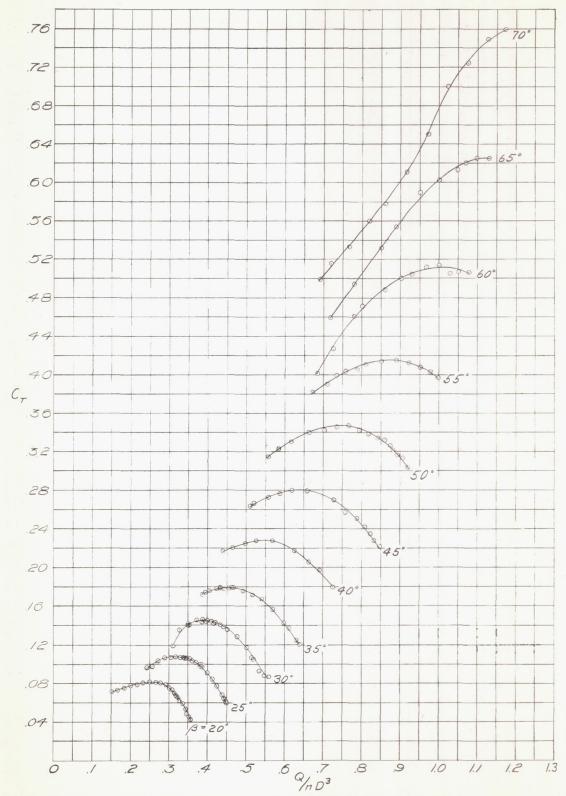
Figure 41.— Torque coefficients. B,24; no contravanes; R.A.F.6 blade section.
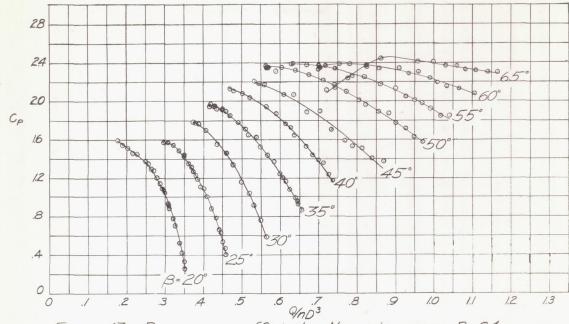
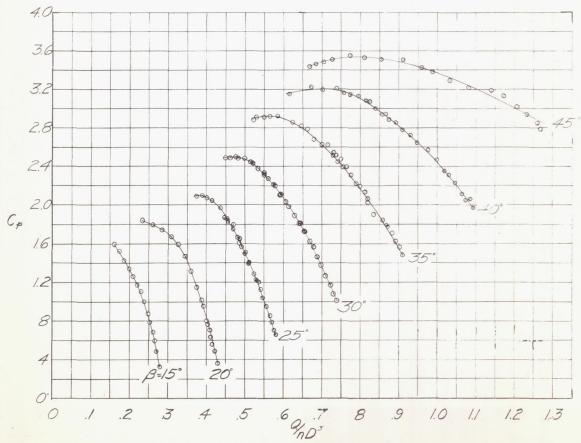Figure 43.- Pressure coefficients. No contravanes; B, 24; NACA 6412 blade section.

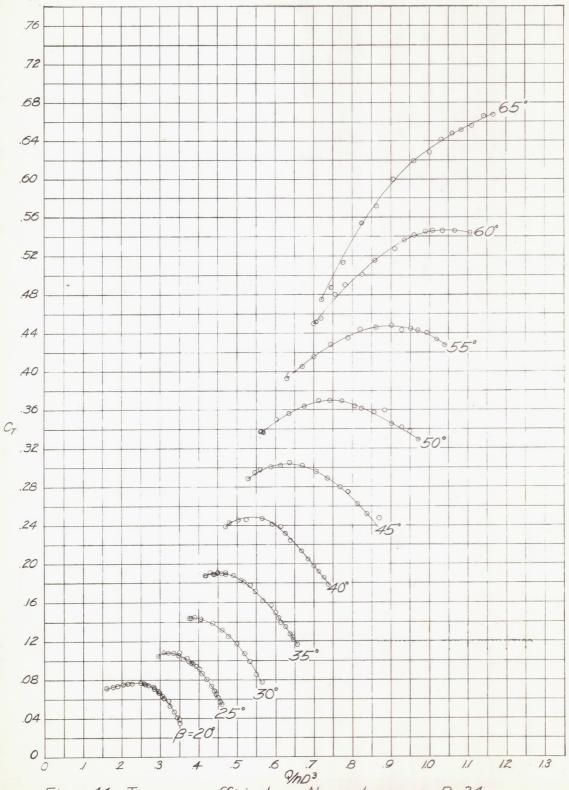Figure 46.- Pressure coefficients. φ, 70; B, 24; NACA 6912 blade section.

Fig. 44

L-304

Figure 44.- Torque coefficients. No contravanes; B, 24;
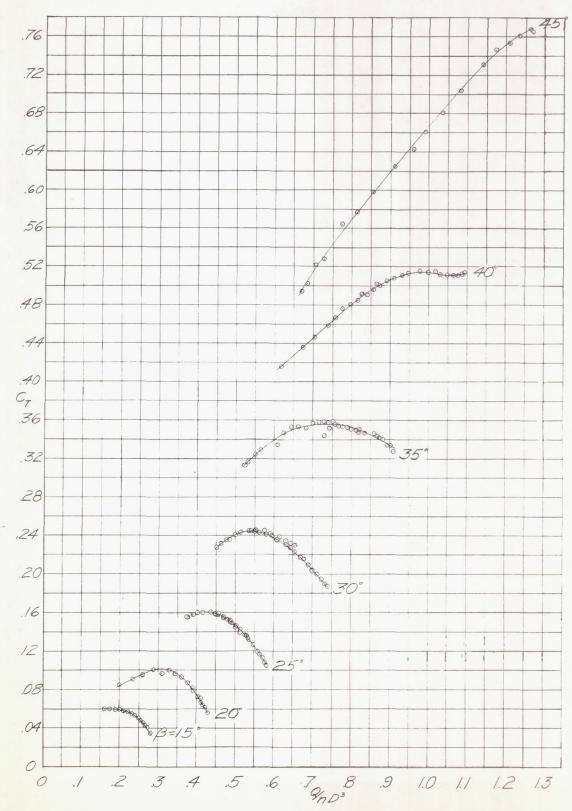NACA 6412 blade section.

Fig. 47

L-304

Figure 47.- Torque coefficients. ϕ, 70°; B, 24; NACA 6412 blade section.
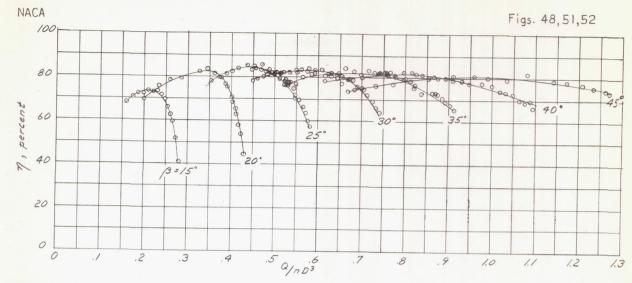
Figure 48.— Axial-fan efficiencies. ϕ, 70°; β, 24; NACA 6412 blade section.
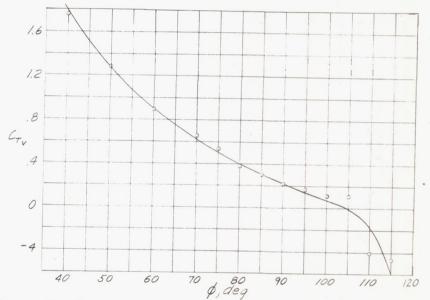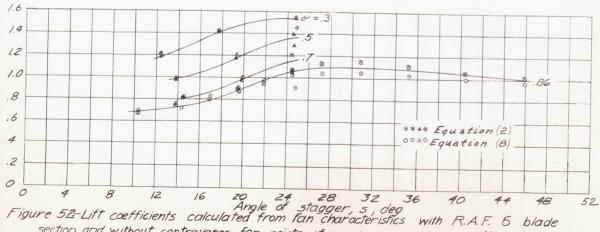
Figure 51.— Contravane torque coefficient.

Figure 52.— Lift coefficients calculated from fan characteristics with R.A.F. 6 blade section and without contravanes for points of maximum pressure coefficients.
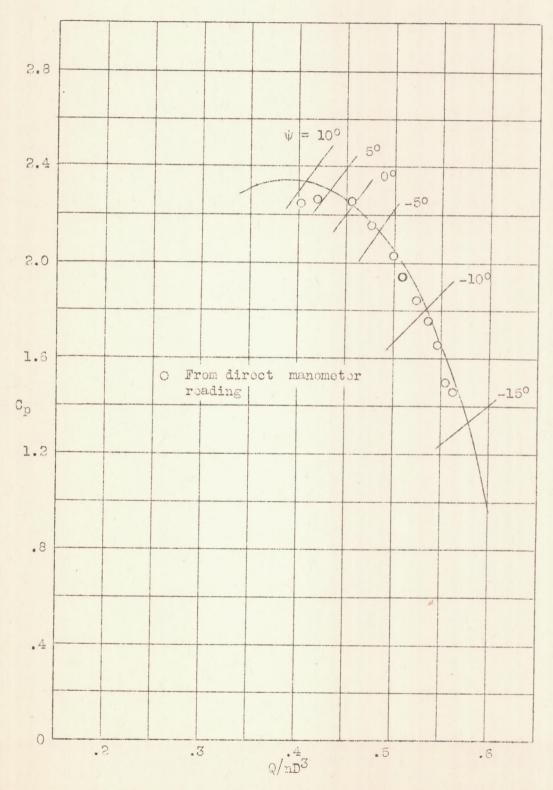
Figure 49.- Comparison of methods of measuring C_p. $\beta = 25^o$, $\phi = 60^o$.

L-304

V   Initial velocity

Contravane forces

$\Delta p_v\, dA$

$\dfrac{dT_v}{r}$

ϕ

α Intermediate
V   velocities

$V\tan\alpha$

Blade forces

$dL\tan\gamma$

dL $\theta+\gamma$

γ $\Delta p_b\, dA$

$\dfrac{dT_b}{r}$

θ

$V\tan\alpha$ $V\tan\psi$
              $\frac{1}{2}V(\tan\alpha-\tan\psi)$

w

β

ψ

α

s

θ

$\pi nD\dfrac{r}{R}$

Blade velocities.
(Velocities are of
blades relative to air)

ψ
V

Final velocities

$V\tan\psi$

Figure 50.—Force and velocity diagrams for blades
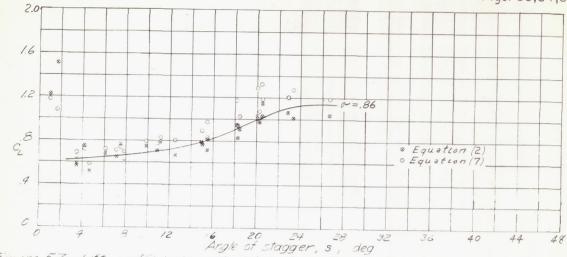   and contravanes of an axial-flow fan.

Figure 53.—Lift coefficients calculated from fan characteristics with R.A.F. 6 blade section and with contravanes for points of maximum pressure coefficient.
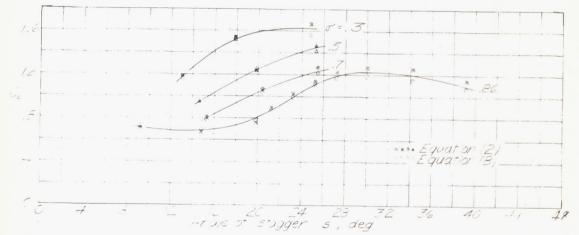

Figure 54.—Lift coefficients calculated from fan characteristics with NACA 6412 blade section and without contravanes for points of maximum pressure coefficient.
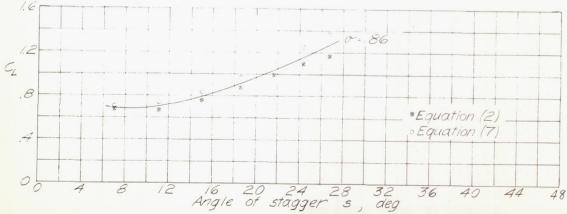

Figure 55.—Lift coefficients calculated from fan characteristics with NACA 6412 blade section and with contravanes for points of maximum pressure coefficient.